

Received 11 February 2024, accepted 1 March 2024, date of publication 4 March 2024, date of current version 14 March 2024.

Digital Object Identifier 10.1109/ACCESS.2024.3373552

## RESEARCH ARTICLE

# Enhancing Household Energy Consumption Predictions Through Explainable AI Frameworks

AAKASH BHANDARY<sup>1</sup>, (Student Member, IEEE), VRUTI DOBARIYA<sup>1</sup>, GOKUL YENDURI<sup>2</sup>,  
RUTVIJ H. JHAVERI<sup>1</sup>, (Senior Member, IEEE), SAIKAT GOCHHAIT<sup>3,4</sup>, (Senior Member, IEEE),  
AND FRANCESCO BENEDETTO<sup>5</sup>, (Senior Member, IEEE)

<sup>1</sup>Department of Computer Science and Engineering, School of Technology, Pandit Deendayal Energy University, Gandhinagar 382007, India

<sup>2</sup>School of Computer Science and Engineering, VIT-AP University, Amaravati, Andhra Pradesh 522237, India

<sup>3</sup>Symbiosis Institute of Digital and Telecom Management, Constituent of Symbiosis International Deemed University, Pune 412115, India

<sup>4</sup>Neurosciences Research Institute, Samara State Medical University, 443079 Samara, Russia

<sup>5</sup>Signal Processing for Telecommunications and Economics, Department of Economics, Roma Tre University, 00154 Rome, Italy

Corresponding author: Francesco Benedetto (francesco.benedetto@uniroma3.it)

The authors would like to gratefully acknowledge the grant GUJCOST/STI/2021-2022/3922 from the Government of Gujarat, India, and support from the Department of Scientific and Industrial Research (DSIR), Government of India under Grant A2KS; Grant number A2KS -11011/7/2022-IRD (SC)- DSIR.

**ABSTRACT** Effective energy management is crucial for sustainability, carbon reduction, resource conservation, and cost savings. However, conventional energy forecasting methods often lack accuracy, suggesting the need for advanced approaches. Artificial intelligence (AI) has emerged as a powerful tool for energy forecasting, but its lack of transparency and interpretability poses challenges for understanding its predictions. In response, Explainable AI (XAI) frameworks have been developed to enhance the transparency and interpretability of black-box AI models. Accordingly, this paper focuses on achieving accurate household energy consumption predictions by comparing prediction models based on several evaluation metrics, namely the Coefficient of Determination ( $R^2$ ), Root Mean Squared Error (RMSE), Mean Squared Error (MSE), and Mean Absolute Error (MAE). The best model is identified by comparison after making predictions on unseen data, after which the predictions are explained by leveraging two XAI frameworks: Local Interpretable Model-Agnostic Explanations (LIME) and Shapley Additive Explanations (SHAP). These explanations help identify crucial characteristics contributing to energy consumption predictions, including insights into feature importance. Our findings underscore the significance of current consumption patterns and lagged energy consumption values in estimating energy usage. This paper further demonstrates the role of XAI in developing consistent and reliable predictive models.

**INDEX TERMS** Energy management, energy forecasting, feature importance, household energy consumption, machine learning models, XAI.

## NOMENCLATURE

*AI* Artificial Intelligence.  
*ANN* Artificial Neural Network.  
*ARIMA* Auto-regression Integrated Moving Average.  
*BiLSTM* Bidirectional Long Short-Term Memory network.

*CatBoost* Categorical Boosting.  
*CBR* CatBoost Regressor.  
*CNN* Convolutional Neural Network.  
*CVOA* Coronavirus Optimization Algorithm.  
*DDS – XAI* Distance-based Data Structures - Explainable AI.  
*DeepLIFT* Deep Learning Input Features.  
*DL* Deep Learning.  
*ELI5* Explain Like I'm 5.  
*GBDT* Gradient Boosting Decision Tree.

The associate editor coordinating the review of this manuscript and approving it for publication was Lei Wang.

<i>LightGBM</i>	Light Gradient Boosting Machine.
<i>LGBMR</i>	LightGBM Regressor.
<i>LIME</i>	Local Interpretable Model-agnostic Explanations.
<i>LR</i>	Linear Regression.
<i>LRP</i>	Layer-wise Relevance Propagation.
<i>LSTM</i>	Long Short-Term Memory network.
<i>MAE</i>	Mean Absolute Error.
<i>ML</i>	Machine Learning.
<i>MSE</i>	Mean Squared Error.
<i>NNGM(1, 1)</i>	Nash Nonlinear Gray Bernoulli Model.
<i>PCC</i>	Pearson Correlation Coefficient.
<i>R<sup>2</sup></i>	R-squared (Coefficient of Determination).
<i>RMSE</i>	Root Mean Squared Error.
<i>RNN</i>	Recurrent Neural Network.
<i>SHAP</i>	SHapley Additive exPlanations.
<i>SVR</i>	Support Vector Regressor.
<i>TBATS</i>	Trigonometric seasonality, Box-Cox transformation, ARIMA errors, Trends, and Seasonal components.
<i>XAI</i>	Explainable AI.
<i>XGBoost</i>	Extreme Gradient Boosting.
<i>XGBR</i>	XGBoost Regressor.

## I. INTRODUCTION

In today's ever-evolving world, effective energy management has become important, enabling us to achieve ambitious sustainability goals, mitigate carbon footprints, and optimize energy costs. Accurate energy forecasting is helpful in empowering households to make informed decisions regarding their energy utilization, to strategically allocate resources, and to actively contribute to the efficient management of energy resources. Nevertheless, traditional statistical methods and time series analysis techniques, while serving as the foundation of forecasting models, often fall short in capturing the dependencies and dynamic patterns inherent in energy consumption data, necessitating the adoption of advanced techniques that are capable of learning these complexities.

Emerging as a powerful tool, artificial intelligence (AI) has proven to be quite useful for energy forecasting, specifically by harnessing machine learning (ML) and deep learning (DL) algorithms to decipher the underlying patterns, interdependencies, and non-linearity within the collected data. However, as these models and algorithms grow increasingly complex, their inherent opacity and lack of interpretability present challenges, hindering our ability to comprehend the factors underpinning their predictions [1]. Within the application of energy forecasting for household usage, the need to illuminate the underlying factors and decipher the complex nature of prediction models holds high significance [2], [3]. However, the intrinsic black-box nature of AI models has raised legitimate concerns in this domain [4]. To address this issue, considerable attempts have been made to develop explainable AI (XAI) techniques and frameworks [5], [6], [7], [8], [9].

In response to the pressing demand for understanding the complex nature of machine learning models, we dig into the area of XAI, a game-changing concept that covers a variety of tools and methodologies aimed at providing AI models with interpretability and transparency [10]. Vital insights into the underlying elements and attributes that are captured by the prediction models can be obtained by incorporating XAI principles into any application. The introduction of XAI frameworks to a black-box model lends it credibility, allowing users to make well-informed judgments based on the model's results.

This paper proposes a ML-based household electric energy consumption prediction methodology that is accurate and explainable with the help of XAI frameworks. We used two established XAI frameworks for interpreting our prediction results: Shapley Additive Explanations (SHAP) [5] and Local Interpretable Model-agnostic Explanations (LIME) [6]. We decided to use these frameworks as they are model-agnostic, i.e., they can generate explanations for any given ML or DL model, along with providing a rich set of plots and graphs to help visualize the explanations. These tools help in identifying the most relevant aspects influencing the models' predictions, effectively bridging the gap between a black-box model and completely transparent predictions.

We chose residential energy usage since most of the previously conducted studies [11], [12], [13], [14] in this area focus primarily on energy usage in the industrial and commercial sectors. While these sectors contribute significantly to overall energy consumption, there is growing awareness that homes play a critical role in overall energy usage patterns. Residential energy consumption accounts for a large share of total energy demand in many regions. Understanding and managing energy consumption at this level, as a result, can have a significant impact on attaining sustainability goals, reducing carbon footprints, and optimizing energy costs. We aim to enable individuals to make better-informed decisions about their energy usage, reduce their environmental impact, and actively contribute to the efficient management of energy resources.

The rest of this manuscript is structured as follows: Section II is dedicated to reviewing related works for energy prediction models and the application of XAI to these models. Section III provides a detailed description of the proposed methodology followed to achieve results. Section IV shows the results and analyses of our experiments. In Section V, we discuss the limitations of this paper, and lastly, Section VI concludes this paper along with future work.

## II. LITERATURE REVIEW AND CONTRIBUTIONS

In recent years, there have been numerous studies on energy forecasting and investigating the application of XAI techniques in various domains, including energy prediction and forecasting. These studies have demonstrated the potential of XAI to enhance the accuracy, reliability, and interpretability of household energy forecasting models. This section covers various studies that employed different energy forecasting

techniques as well as papers that implemented different XAI techniques for forecasting models.

### A. STUDIES ON ENERGY FORECASTING TECHNIQUES

In this research [12], Hu examined a neural-network-based grey forecasting approach, specifically the Nash Nonlinear Gray Bernoulli Model (NNGM (1,1)), for the prediction of power consumption. The NNGM (1,1) model improved on standard grey forecasting by addressing challenges associated with identifying the development coefficient and control variable. The primary contributions of the research included establishing the effectiveness of the NNGM (1,1) model in predicting power consumption using restricted sample data and comparing the NNGM (1,1) model to other forecasting methodologies. However, the research has flaws, such as the lack of a discussion of the NNGM (1,1) model's application to domains other than electricity consumption prediction and the lack of an in-depth analysis of potential downsides or limits connected with the NNGM (1,1) model.

Divina et al. [15] suggested an ensemble learning technique for anticipating short-term electric energy use. To improve forecast accuracy, they developed an ensemble approach that combines regression trees, evolutionary computation, random forests, and artificial neural networks with gradient boosting. Some approaches, however, excelled at short-term forecasts but were prone to overfitting. Also, the computational complexity and training time of the ensemble technique, particularly for gradient boosting, might encounter difficulties.

Torres et al. [16] offered an optimized Long Short-Term Memory network (LSTM) model for accurate electricity consumption forecasting in Spain. They identified ideal hyperparameters using a combination of random search and the proposed Coronavirus Optimization Algorithm (CVOA) while minimizing prediction error. Comparing the LSTM model to older methods proved its greater ability to capture complicated consumption patterns. While generalizability in other regions is still an issue, this study indicates the LSTM model's effectiveness in improving electricity demand forecasting.

Divya et al. [17] proposed an artificial intelligence approach to enhance time series forecasting for energy consumption. They explored various forecasting methodologies, including the Auto-regression Integrated Moving Average (ARIMA) and 'Trigonometric seasonality, Box-Cox transformation, ARIMA errors, Trends, and Seasonal components' (TBATS) models, with the latter exhibiting the highest accuracy in managing multiple seasonalities or temporal patterns. The study also introduced a novel data collection technique involving a custom-built sensor array and a cloud database for visualization and testing, shedding light on energy consumption patterns. However, the study does not focus on the interpretation of the results obtained by the models.

The above discussed studies are summarized in Table 1. Even though AI models are excellent at predicting and

**TABLE 1. Summary of studies on energy forecasting techniques.**

Reference	Technologies Used	Contributions	Limitations
[12]	NNGM (1,1) Model	Improved power consumption prediction using NNGM (1,1) model. Comparison with other methods.	Limited application discussion. Lack of in-depth downside analysis.
[15]	Ensemble Learning	Developed ensemble approach for electric energy use prediction, improving accuracy.	Potential overfitting. High computational complexity and training time.
[16]	Optimized LSTM Model	Optimized LSTM model for electricity consumption forecasting. Improved accuracy in capturing patterns.	Limited generalizability to other regions.
[17]	ARIMA, TBATS Models	Explored ARIMA and TBATS models for energy consumption forecasting. Introduced novel data collection technique.	Limited focus on results interpretation.

forecasting, one of their primary limitations is the lack of transparency and justification for the predicted results. XAI techniques help bridge this gap, for which we reviewed a few relevant studies.

### B. STUDIES ON XAI TECHNIQUES FOR FORECASTING MODELS

Schlegel et al. [13] explored the use of various XAI techniques such as LIME, Layer-wise Relevance Propagation (LRP), Deep Learning Input Features (DeepLIFT), Saliency Maps, and SHAP on various time-series datasets using Convolutional Neural Network (CNN) and Recurrent Neural Network (RNN) architectures. Their results show that SHAP consistently performs well across different models, while DeepLIFT and LRP exhibit the largest decrease in overall quality metrics. However, the study acknowledges certain limitations, including the number of XAI methods considered and the use of a small number of datasets for the study to be comprehensive and all-encompassing.

Kuzlu et al. [14] presented a comprehensive study on gaining insights into forecasting solar photo-voltaic power generation using explainable AI techniques. The authors employed the RFR model and applied XAI frameworks including LIME, SHAP, and Explain Like I'm 5 (ELI5)

to interpret the predictions. Their results demonstrate the effectiveness of the frameworks in providing insights into the predictions and identifying relevant parameters. However, the study does not compare the Random Forest Regressor (RFR) model with other prediction methods.

Thrun et al. [18] proposed a framework, Distance-based Data Structures - XAI (DDS-XAI), for multivariate hydro-chemical time series analysis. The framework uses topographic map visualization and projection-based clustering to identify meaningful structures in the data. The study demonstrated the application of the framework on three datasets and extracted relevant explanations using decision trees. The results showed that the framework can provide interpretable insights into water quality predictions. The study does, however, acknowledge certain limitations, such as the limited availability of the data and the need for careful selection of distance metrics.

Sim et al. [11] presented a unique approach for variable selection in energy forecasting models. The authors utilized Support Vector Regressor (SVR), Extreme Gradient Boosting (XGBoost), Light Gradient Boosting Machine (LightGBM), long-LSTM, and the SHAP framework to identify relevant input factors using energy data from a university building in Seoul. The results demonstrated that models incorporating 'Strong' and 'Strong and Ambiguous' variables outperformed others by categorizing variables based on their influence. The study is limited to a restricted data collection period and the use of only one XAI method for analyzing the predictions.

These studies, as summarized in Table 2 offer valuable insights into the application of XAI frameworks for forecasting models in various industrial and commercial settings. However, little focus has been devoted to the prediction and explanation of energy consumption patterns in residential buildings.

Based on the shortcomings of traditional AI methods and insights gained from the papers covering XAI techniques, our objective was to develop a household energy consumption prediction workflow by incorporating high-performing ML and DL algorithms. Furthermore, we aimed to leverage XAI techniques to enhance the interpretability of predictions, contributing to a more transparent and understandable energy forecasting system.

The primary contributions of this paper are summarized as follows:

- The introduction of an accurate and efficient explainable prediction workflow utilizing ML models, and the LIME and SHAP XAI frameworks.
- Evaluation of the applied models using relevant metrics - Root Mean Squared Error (RMSE), Coefficient of Determination ( $R^2$ ), Mean Squared Error (MSE), and Mean Absolute Error (MAE), using a separate validation set and an unseen testing set.
- Analysis of explanations generated by LIME and SHAP in local (individual instance) and global scope using plots and visualizations provided by the frameworks.

**TABLE 2.** Summary of studies on XAI techniques for forecasting models.

Reference	Technologies Used	Key Contributions	Limitations
[13]	Various XAI Techniques, CNN, RNN	Evaluation of XAI methods on time-series data. SHAP performs consistently well.	Limited number of XAI methods considered, small dataset usage.
[14]	RFR, XAI Frameworks (LIME, SHAP, ELI5)	Insights into solar PV power generation using RFR and XAI frameworks.	Lack of comparison with other prediction methods.
[18]	DDS-XAI, Topographic Maps, Clustering	Framework for interpretable insights into multivariate hydro-chemical time series.	Limited dataset availability, distance metric selection.
[11]	SVR, XGBoost, LightGBM, LSTM, SHAP	Variable selection in energy forecasting. Models incorporating Strong variables outperform.	Restricted data collection period, use of one XAI method.

### III. METHODOLOGY

This section describes the methodological approach followed in this work. We started by sampling and preprocessing electrical energy consumption data, followed by comparison and selection of prediction models, evaluation of the models using various metrics, and application of XAI frameworks to interpret the model predictions. Fig 1 shows a visual overview of the methodology.

#### A. DATA COLLECTION

For this study, a dataset of household electric energy consumption collected by the authors of the paper [17] was used. We used this data since it was not collected in a controlled environment, but was collected from the authors' apartments located in Bangalore, India, with the help of smart meters. It also accurately portrays the pattern of household energy consumption following the COVID-19 pandemic. The energy consumption trend has been shown in Fig 2. The dataset consists of consumption data for a three-phase electricity supply, with records at an interval of every 7 seconds. The high-load appliances consuming electricity include air conditioners, geysers, washing machines, and a refrigerator. The data spans the time period from 6<sup>th</sup> April 2021 to 17<sup>th</sup> August 2021. For our study, we focused on Phase 1 electricity consumption and sampled the same from the original dataset.

All the existing and engineered features (attributes) of the dataset are described in Table 3.

#### B. DATA PREPROCESSING

A sampling interval of 20 minutes was chosen to accurately capture the consumption information. Firstly, outlier



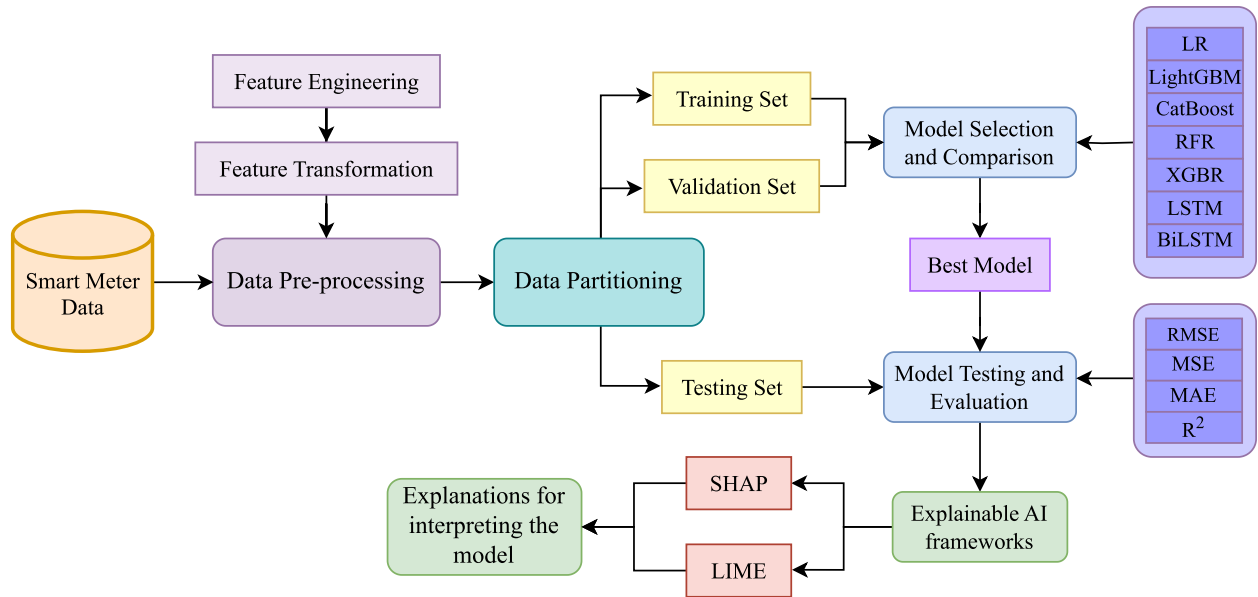


FIGURE 1. Methodology.

values were discarded using the interquartile range (IQR) method [19]. This was done to ensure consistency and reliability across the modeling and explanation process. The upper and lower bounds for the IQR were kept as the 95<sup>th</sup> and 15<sup>th</sup> percentiles, respectively, since only extreme outliers were observed.

Min-max scaling was performed on all the features to convert them to a scale of 0.0 to 1.0 as it guarantees consistency in scales and distributions among variables [20]. It is especially important for models that are sensitive to feature sizes, such as linear regression and neural networks. Equation (1) defines the min-max scaling process, where  $X$  is the feature vector,  $X_{scaled}$  is the scaled feature vector, and  $X_{max}$  and  $X_{min}$  are the maximum and minimum values of the specified feature vector.

$$X_{scaled} = \frac{X - X_{min}}{X_{max} - X_{min}} \quad (1)$$

The *hour\_interval*, and *day* features were transformed using a circular transformation by converting them to angles in radians [22] using:

$$i_{new} = 2\pi \cdot \frac{i}{n} \quad (2)$$

In (2),  $i$  represents a specific instance and  $n$  is the total number of unique values in the feature. This process ensures that the cyclic nature of time is appropriately encoded, allowing the model to capture daily patterns and periodic variations in energy consumption more accurately. This method is especially helpful for linear models and neural networks to handle circular relationships and for better modeling of the cyclic behavior of the feature. This also ensures a fair testing environment for comparing different models.

TABLE 3. Description of all the features in the dataset.

Feature	Description	Unit
<i>time</i>	Time-stamp of the observation	-
<i>day</i>	Day of the month	-
<i>current</i>	Average current consumed in the 20-minute interval	Ampere (A)
<i>voltage</i>	The voltage of electricity supply	Volts (V)
<i>power</i>	Average power consumed in the 20-minute interval	Watt (W)
<i>frequency</i>	Frequency of the electricity supply	Hertz (Hz)
<i>pf</i>	The power factor of the household	-
<i>energy</i>	Cumulative energy consumed till a specific instance	Watt-hour (Wh)
<i>inst_energy_t-1</i>	Energy consumed in the previous 20-minute interval [21]	Wh
<i>hour_interval</i>	Numerical value indicating the 20-minute interval within an hour	-
<i>inst_energy</i>	Target feature; average energy consumed in a 20-minute interval	Wh

To train, verify, and test the models, we separated the dataset into training, testing, and validation sets, with a 70%-15%-15% split respectively. The splitting was performed without shuffling to retain the time-series nature of prediction.

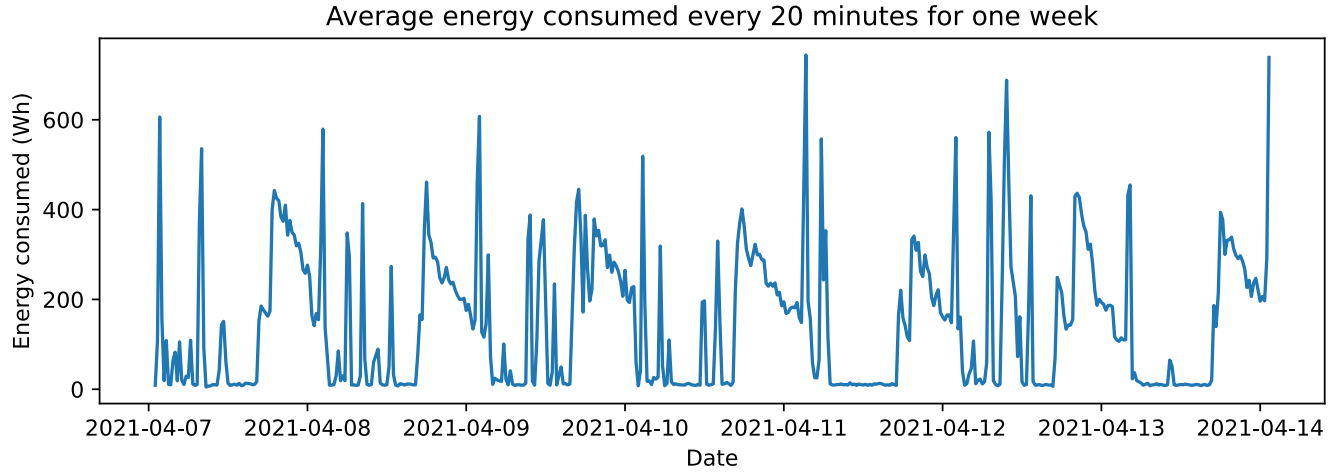


**FIGURE 2.** Average energy consumption of every 20 minutes (in kWh) for one week, depicting the trend followed by the target variable.

### C. FEATURE ENGINEERING

New features were computed using pre-existing features in the dataset. For this process, the Pandas [23] and Numerical Python (NumPy) [24] libraries were utilized. All the engineered features are described below:

- *inst\_energy*: This feature was calculated using the *energy* feature by subtracting the previous cumulative energy value from the current instance.
- *inst\_energy\_t-1*: This column contains the lagged value of the *inst\_energy*, which is generated by shifting the *inst\_energy* values by one time step to represent the value of the  $t-1^{\text{th}}$  instance. This was done to study the temporal dependency of consumption patterns.
- *day*: The *day* attribute was extracted from the *time* using attributed provided in Pandas for a 'datetime' object.
- *hour\_interval*: This was calculated using the *hour* and *minute* attributes of the *time* feature. The feature value signifies which third of any given hour (since the sampling interval is 20 minutes) the data point belongs to.

Since the data only spans 133 days, we did not extract 'month' or 'year' features as there was simply not enough data to reveal a monthly or yearly usage pattern.

### D. FEATURE SELECTION

We discarded some of the features of the dataset before model implementation based on factors such as their relevance to the prediction task and the potential for introducing temporal dependencies. Moreover, the Pearson correlation coefficient (PCC) [25] of all the features with the target was also considered for feature selection.

The PCC described in (3) measures the strength and direction of a linear relationship between two features. It ranges from  $-1$  to  $1$ , where a correlation coefficient of  $1$  indicates a perfect positive relationship, and  $-1$  indicates perfect negative relationship. The calculated correlation

Correlation coefficient of all features with the target.

current	0.85
power	0.85
pf	0.71
inst_energy_t-1	0.64
frequency	0.05
day	0.0093
minute	0.0044
hour_interval	-0.058
hour	-0.058
energy	-0.29
time	-0.29
voltage	-0.34
inst_energy	

**FIGURE 3.** Calculated PCCs for all features.

coefficients for all features are shown in Fig 3.

$$\rho = \frac{\sum_{i=1}^n (x_i - \bar{x})(y_i - \bar{y})}{\sqrt{\sum_{i=1}^n (x_i - \bar{x})^2 \sum_{i=1}^n (y_i - \bar{y})^2}} \quad (3)$$

Here,  $x$  and  $y$  are the two feature vectors, and  $\bar{x}$  and  $\bar{y}$  are the arithmetic means of the two vectors.

Since the task was to predict the average energy consumed during a given time interval based on other parameters, the *inst\_energy* column was identified as the target feature.

The *energy* feature was discarded as it stored cumulative energy consumption information. Cumulative data can introduce unwanted temporal dependencies and make it challenging to make accurate predictions. The *power* feature was not used as it can be derived using the *current* and *voltage*

values at a given instance. Also, the calculated PCC of *current* with *power* was 1, whereas, both have a PCC of 0.85 with the target. This makes keeping both features redundant, and the removal of one simplifies the feature set. The *time* feature was dropped as all relevant temporal dependencies are captured in the *day* and *hour\_interval* features. Moreover, the *time* variable is of the 'datetime' type, which is not directly ingestible by most predictive models. The *hour* and *minute* features were also discarded as this information was already combined in *hour\_interval* feature. This decision is also justified by the observation that the PCC of *hour* with *hour\_interval* is 1, whereas both have a PCC of  $-0.058$  with the target.

### E. COMPARISON AND SELECTION OF PREDICTION MODELS

A range of prediction models were selected for comparison and testing based on their specific capabilities to address various aspects of the prediction task.

Linear Regression (LR) and Random Forest Regressor (RFR) [26] were implemented using the open-source Scikit-learn Python library. Two neural network models, namely Long Short Term Memory (LSTM) and Bidirectional Long Short Term Memory (BiLSTM) networks [27] were implemented using the open-source TensorFlow Python library. Additionally, the LightGBM Regressor (LGBMR) [28], CatBoost Regressor (CBR) [29], and XGBoost Regressor (XGBR) [30] were implemented using their respective open-source Python libraries. Each of these models was selected for specific reasons: LR served as a baseline estimator, and LSTM and BiLSTM were chosen for their suitability for time-series data. RFR, along with the three Gradient Boosting Decision Tree (GBDT) models (LGBMR, CBR, and XGBR), were considered due to their ability to capture complex non-linear relationships within the data [31], [32], which can be particularly advantageous in predictive tasks involving intricate patterns.

The models were trained on the training set after hyperparameter tuning using GridSearchCV.

#### 1) HYPERPARAMETER TUNING

The trainable parameters (hyperparameters) of the models were tuned using the grid search with cross-validation (GridSearchCV).

For LR, the *fit\_intercept* parameter, which decides whether the model will calculate the intercept term (the predicted value when all input variables are zero) is set to True by default.

For RFR, the *n\_estimators* parameter controls the number of trees in the ensemble. The *min\_samples\_split* parameters controls the minimum number of data points (samples) required to split an internal node of each tree. The *max\_features* parameters is used to decide the number of features in the data to be considered for the best split. The best hyperparameters resulted using GridSearchCV were:

{*n\_estimators*: 25, *min\_sample\_split*: 4, *max\_features*:  $\log_2$ }.

For LGBMR, CBR, and XGBR, four hyperparameters each were tuned. The *n\_estimators* parameter controls the number of boosting rounds performed by the ensemble. The *max\_depth* parameter controls the depth of each tree in the ensemble (a value of  $-1$  indicates unrestricted depth). The *learning\_rate* parameter controls the rate of weight updates of the model, and the *reg\_lambda* parameter controls the L2 regularization term [33], which helps prevent overfitting. The best resultant values for each model were:

- LGBMR: {*n\_estimators*: 100, *max\_depth*:  $-1$ , *learning\_rate*: 0.1, *reg\_lambda*: 0.0}
- CBR: {*n\_estimators*: 200, *max\_depth*: 7, *learning\_rate*: 0.1, *reg\_lambda*: 5}
- XGBR: {*n\_estimators*: 25, *max\_depth*: 5, *learning\_rate*: 0.1, *reg\_lambda*: 1}

The LSTM and BiLSTM models were constructed having an input layer of 16 neurons, two hidden layers with 16 and 8 neurons respectively, and one fully connected output layer having one neuron for continuous output. The Adam optimization technique [34] was used to tune both the models, and an initial learning rate of 0.001 was found optimal. Early stopping based on the validation loss was implemented in order to prevent overfitting.

Finally, all models were evaluated using the unseen testing set and various evaluation parameters, and the best estimator was chosen for further analysis using XAI frameworks to gain insights into the predictions.

### F. METRICS FOR MODEL EVALUATION

The fine-tuned models were evaluated on the validation and testing sets using standard evaluation parameters discussed below:

- 1) Root Mean Squared Error: The RMSE measures the square root of the mean of the squared difference between the actual and predicted values. It is calculated using:

$$RMSE = \sqrt{\frac{1}{n} \sum_{i=1}^n (y_i - \hat{y}_i)^2} \quad (4)$$

- 2) Mean Squared Error: The MSE measures the mean of the squared difference between the actual and predicted values. It is calculated using:

$$MSE = \frac{1}{n} \sum_{i=1}^n (y_i - \hat{y}_i)^2 \quad (5)$$

- 3) Mean Absolute Error: The MAE quantifies the meaning of the absolute difference between the actual and predicted values. It is calculated using:

$$MAE = \frac{1}{n} \sum_{i=1}^n |y_i - \hat{y}_i| \quad (6)$$

- 4) Coefficient of Determination: The  $R^2$  measures the proportion of the variance in the dependent variable that is explained by the independent variables. It is used to quantify the goodness of fit of a regression model. It is calculated using:

$$R^2 = 1 - \frac{\sum_{i=1}^n (y_i - \hat{y}_i)^2}{\sum_{i=1}^n (y_i - \bar{y})^2} \quad (7)$$

In (4), (5), (6), and (7),  $n$  is the length of the array of actual values,  $y$  is the array of actual observed values,  $\hat{y}$  is the array of predicted values, and  $\bar{y}$  is the mean of the actual values.

We emphasized on RMSE [35] and  $R^2$  [36] as they provide a concise measure of how well the model's predictions match the actual variance in the data, aiding in assessing the overall predictive capability of the models.

### G. XAI FRAMEWORKS USED

We employed the LIME and SHAP frameworks to understand the predictions made by the models. Both of these frameworks are model-agnostic, meaning that they can generate explanations for any ML or DL model. Moreover, both frameworks are well documented and provide an extensive choice of plots and visualizations that make it easier to understand the explanations. The explanations provided by these two frameworks help bridge the gap between these complex AI models and human understanding by providing important information about feature importance, individual predictions, and even model behavior.

#### 1) LIME

The model-agnostic LIME framework is useful for explaining predictions that work on individual predictions by approximating the behavior of a black-box model in a local region around a specific instance [6]. It is primarily used to provide local explanations that focus on the features that are most influential for a specific prediction instance. This is particularly useful for understanding cases where the prediction is inaccurate or mis-classified in classification tasks. LIME provides an explanation for an instance as follows:

$$\xi(x) = \operatorname{argmin}_{g \in G} \mathcal{L}(f, g, \pi_x) + \Omega(g) \quad (8)$$

Here,  $G$  is the set of models considered interpretable,  $\Omega(g)$  is a measure of complexity of any explanation  $g \in G$ ,  $f$  is the model being explained,  $\pi_x$  is used to define the locality (distance) of other instances around  $x$ , and  $\mathcal{L}(f, g, \pi_x)$  is the measure of how accurate  $g$  is in comparison to  $f$ . The goal of LIME is to minimize  $\mathcal{L}(f, g, \pi_x)$  in order to obtain the closest possible interpretable approximation of a black-box model.

#### 2) SHAP

The model-agnostic SHAP framework works by calculating Shapley values for each feature used by the model. From the perspective of cooperative game theory, Shapley values are quantities that measure the contribution or importance of each

**TABLE 4. Comparison of evaluation metrics for the regression models on the testing data.**

Model	RMSE	MSE	MAE	$R^2$
LGBMR	0.0635	0.0040	0.0207	0.7538
CBR	0.0645	0.0042	0.0216	0.7458
BiLSTM	0.0651	0.0042	0.0273	0.7415
RFR	0.0653	0.0043	0.0232	0.7393
XGBR	0.0655	0.0043	0.0273	0.7380
LSTM	0.0667	0.0044	0.0285	0.7279
LR	0.0692	0.0048	0.0244	0.7072

player in a cooperative game [37]. This has been adapted in the context of explainable AI to quantify the contribution of features in AI models [5].

$$\phi(i) = \sum_{S \subseteq N \setminus \{i\}} \left[ \frac{|S|!(|N| - |S| - 1)!}{|N|!} \right] [f(S \cup \{i\}) - f(S)] \quad (9)$$

Equation (9) defines the Shapley value  $\phi(i)$  which is the average contribution of feature  $i$  to all possible combinations of features,  $N$  is the set of all features,  $S$  is a subset of features excluding feature  $i$ ,  $|S|$  represents the number of features in set  $S$ ,  $|N|$  is the total number of features,  $f(S)$  is the prediction made by the model when considering only the features in  $S$ , and  $f(S \cup \{i\})$  represents the model's prediction when a feature  $i$  is added to  $S$ .

The Shapley value is calculated for each feature, providing an explanation of the model's predictions by attributing contributions to each feature.

## IV. RESULTS AND DISCUSSION

In this section, we present the prediction results achieved by the models and compare them. We also interpret the prediction results using explanations generated by LIME and SHAP.

Testing results show that LGBMR performed better than all other models, followed closely by CBR, BiLSTM, RFR, XGBR, and LSTM, whereas LR performed the poorest. XGBR showed the fastest training times with an average of 22.75 ms for five independent training rounds. It was followed by LGBMR with 61.99 ms, RFR with 308.35 ms, LR with 487.85 ms, and CBR with 513.09 ms. Both the LSTM and BiLSTM were prone to overfitting and took between 30 to 75 seconds to train for a maximum of 100 epochs. This is most likely due to the limited amount of available data as neural networks demand a high amount of data for better generalizability.

### A. PERFORMANCE OF MODELS

on testing data The final test prediction results produced by all the models are summarized in Table 4. It can be observed that the tuned LGBMR performed better than all other models



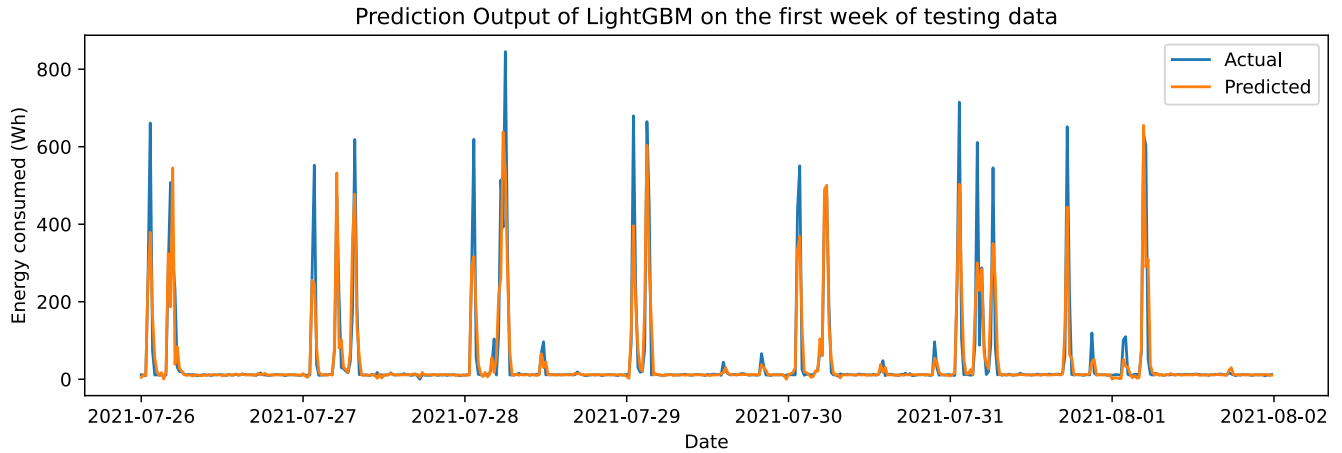


FIGURE 4. Prediction output of LGBMR in the first week of the testing data.

with a  $R^2$  of 0.7538. This means that the model was able to account for 75.38% of the variability in the testing data. The model resulted in an RMSE of 0.0635. Fig 4 shows the line plot for actual and predicted testing instances. It can be observed that the model struggled to predict peak values of energy consumption. This can be explained due to the stark difference in the sequential arrangement of the training (given in Fig 2) and the testing data. Visual comparisons of RMSE and  $R^2$  for each tested model are shown in Fig 5 and Fig 6 respectively. It is observed that LSTM is a slightly higher improvement over LR, and LGBMR is a slightly higher improvement over CBR as compared to the improvements by other models.

### 1) LightGBM

The LightGBM framework is an implementation of the GBDT class of ML models. It was designed to perform better than existing GBDT implementations such as XGBoost. It uses a combination of histogram-based tree building and exclusive feature bundling [28] to build ensembles of shallow decision trees while having shorter training times and higher accuracy than other similar models. Algorithm 1 provides a simplified pseudo-code for the ensemble technique used in the LightGBM framework.

While the PCC gives a statistical measure of the strength and direction of relationship between features and can be used for feature selection, it does not inherently indicate the importance of features in the context of prediction. Moreover, an in-depth analysis of the predictions is often limited with most models being ‘black-box’ in nature. Hence, XAI methods are important, enabling analysis of the model predictions on both a global and a local scope. The results of XAI analysis are presented below.

### B. USING LIME TO INTERPRET LGBMR PREDICTIONS

Fig 7 displays the LIME tabular explainer plots for individual predictions made by the model. From left to right, the LIME plots consist of three parts: The predicted value of the target,

### Algorithm 1 Ensemble Building Algorithm Used by LightGBM.

```

1: Initialize: nodeSet  $\leftarrow \{0\}$ , rowSet  $\leftarrow \{\{0, 1, 2, \dots\}\}$ 
2: for t  $\leftarrow 1$  to num_trees do
3:   for i  $\leftarrow 1$  to d do do
4:     for node in nodeSet do
5:       usedRows  $\leftarrow$  rowSet[node]
6:       for k  $\leftarrow 1$  to m do do
7:         H  $\leftarrow$  new Histogram()
8:         for j in usedRows do do
9:           bin  $\leftarrow$  I.f[k][j].bin
10:          H[bin].y  $\leftarrow$  H[bin].y + I.y[j]
11:          H[bin].n  $\leftarrow$  H[bin].n + 1
12:        end for
13:        best_split  $\leftarrow$  find_best_split(H)
14:        update_tree(node, best_split)
15:        update_rowSet(node, best_split)
16:      end for
17:    end for
18:  end for
19:  boosting_update()
20:  add_tree_to_ensemble()
21: end for

```

the bar chart at the center depicting the influence of each feature on that particular predicted instance, and the values of each feature of that instance. A positive influence indicates that an increase in the value of the attribute resulted in the prediction value being pushed higher than the base value. A negative influence means that the prediction was pushed higher when the feature value decreased. The values assigned to each feature quantify the extent of influence.

It can be observed that for both the instances, the *current* and *inst\_energy\_t-1* are the top two contributors having a positive influence on the prediction in descending order. These two features have more influence over the prediction than the rest which can be seen from the feature importance

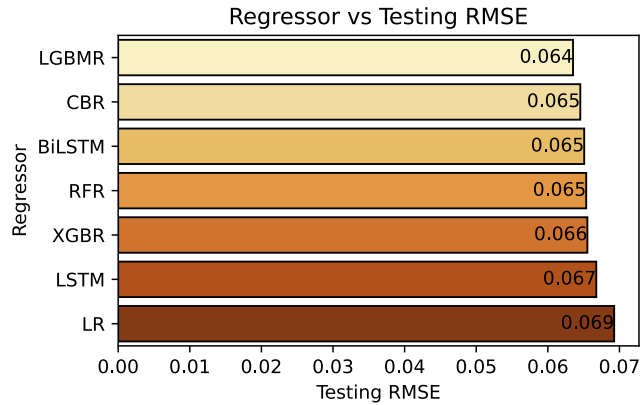


**FIGURE 5.** Visual comparison of RMSE values of the models on the testing data.

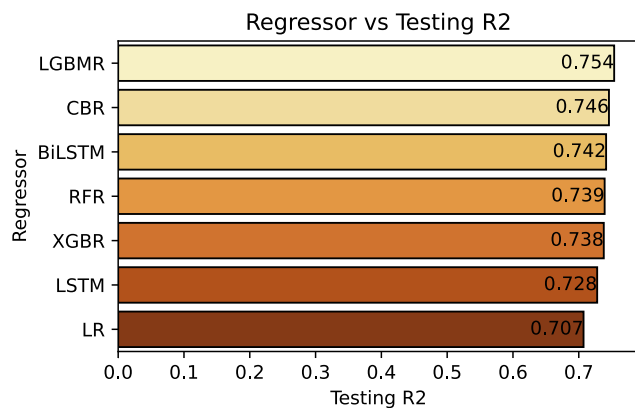


**FIGURE 6.** Visual comparison of  $R^2$  values of the models on the testing data.

coefficients assigned by the LIME tabular explainer. For the first instance, *voltage* and *hour\_interval* stood out as the least influential features, whereas for the second instance they were *day* and *pf*. It is to be noted that since LIME generates an approximation of the model by only considering the locality of the selected instance, the results obtained may vary from instance to instance, and from experiment to experiment.

The LIME feature importance plot for the instance considered in Fig 7(a) is given in Fig 8. From this, it clearly observable that *current* and *inst\_energy\_t-1* have a much higher contribution than the other features. The high influence of *current* is supported by its PCC with *inst\_energy*, which is 0.85. The high influence of *inst\_energy\_t-1* can be explained as the feature contains lagged values from the previous time step of the target *inst\_energy* feature. This means that the temporal pattern followed by energy consumption is well captured by LGBMR.

### C. USING SHAP TO INTERPRET LGBMR PREDICTIONS

For analyzing the prediction results using SHAP, we used the beeswarm and waterfall plots. The beeswarm plot shown in Fig 9 summarizes the influence of each feature for the entire prediction array, i.e., it provides a global explanation

of the model. It can be observed that according to SHAP, and in alignment with LIME, the *current* and *inst\_energy\_t-1* features are the top influencers. The plot shows that higher values of both features have a high positive influence over the predictions, while lower values have a moderate negative influence. This means that higher values of both features are likely to result in higher values being predicted, while lower values are likely to result in lower predictions. It can also be observed from the figure that the target feature does not have a clear dependence on features other than *current* and *inst\_energy\_t-1*.

The waterfall plots for two individual prediction instances are given in Fig 10. For both the the explained instances, *current* and *inst\_energy\_t-1* features are the top influencers. The waterfall plot starts from a baseline value, which is the expected value of the target variable  $E[f(X)]$ , and plots the magnitude of influence of each independent feature (the SHAP value). The features are arranged from least influential to most influential. The predicted value  $f(x)$  of a particular instance  $x$  can be calculated by adding the raw SHAP value of each feature to the baseline value moving up the vertical axis starting from the least influential feature. It can be observed that for the first instance (Fig 10(a)), *current* had a positive influence, while for the second instance (Fig 10(b)), it had a negative influence. This suggests that the first instance encountered a higher value of the feature, while the second instance observed a lower value. A similar variation in the direction of contribution can be observed for *inst\_energy\_t-1* as well.

The effect of *current* and *inst\_energy\_t-1* on the target, i.e. *inst\_energy* can also be studied from the SHAP dependence plots given in Fig 11. The dependence plots contain the values of the feature-of-interest on the x-axis, and its SHAP values on the y-axis. The points in the plot are color coded based on the value of another feature, which is *inst\_energy* in our case. It can be seen that both the features are related with the target in a positive and mostly linear correlation pattern.

### D. EXPERIMENTAL SETUP

All experiments performed for this study were implemented using Python version 3.11 on a system with an AMD(R) Ryzen(TM) 5 4500U @ 2.3 GHz processor and 16 GB RAM.

### E. DISCUSSION

The results obtained by the LGBMR underscore the effectiveness of GBDT models for the application of household energy consumption prediction. An observation can be made from Fig 6 that while LGBMR emerged as the best model, the alternative GBDT models - XGBR and CBR - and RFR exhibited their robustness and suitability for this task. This underscores the versatility of GBDTs and Random Forests, offering flexibility depending on the area of application.

Furthermore, the analysis of explanations given by LIME and SHAP reveals valuable insights into the factors driving the model's predictions. *current* and *inst\_energy\_t-1* are consistently identified as the top contributors by both

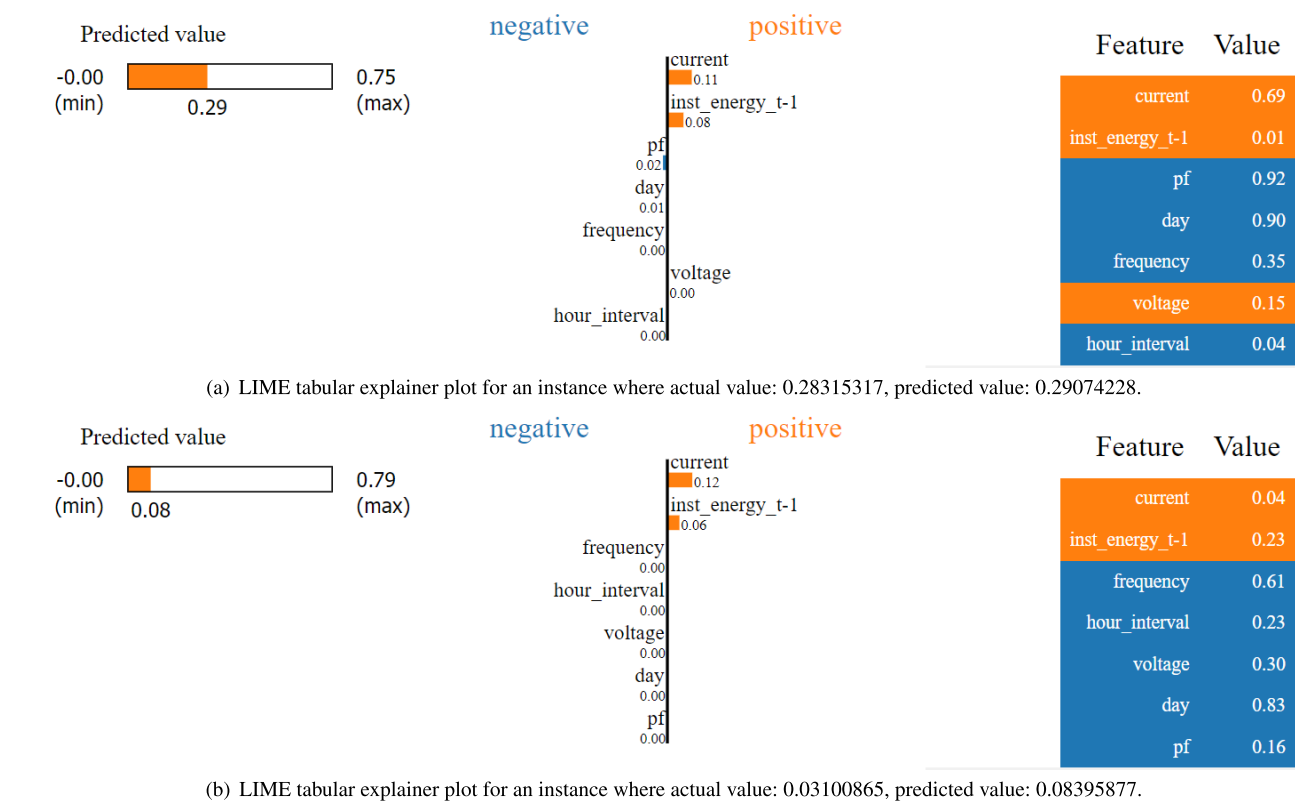


FIGURE 7. LIME tabular explainer plots for interpreting individual predictions of the LGBMR.

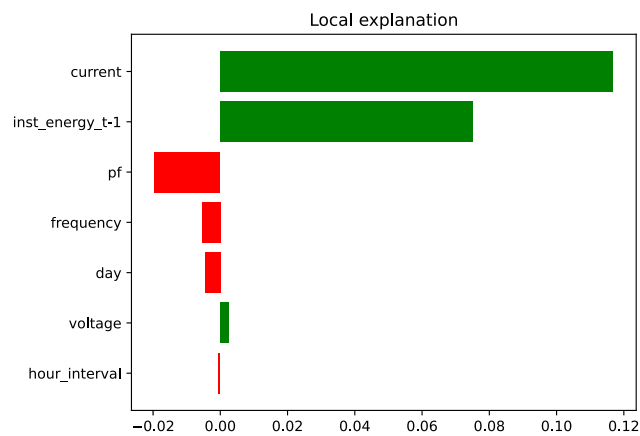


FIGURE 8. LIME feature importance plot for an instance where actual value: 0.28315317, predicted value: 0.29074228.

the frameworks. This finding not only confirms the high correlation between *current* and the target *inst\_energy* but also highlights the temporal dependencies captured by the *inst\_energy\_t-1* in predicting energy usage. However, in comparison to the two top contributors, the rest of the features have very little influence over the predictions.

In our work, an emphasis is laid on enhancing the transparency and interpretability of model predictions by using XAI frameworks. While there are multiple software tools on the market that provide accurate predictions, our

workflow using LIME and SHAP enables users to understand the driving factors behind predictions. The XAI insights are particularly valuable for small buildings or family homes, as they provide information that facilitates well-informed decisions for optimizing energy consumption patterns.

V. LIMITATIONS AND THREATS TO VALIDITY

In this section, we discuss the limitations and potential threats to validity encountered during the course of our study, which include:

- 1) This study focuses on the electric energy consumption of a single household. The findings of this work may not generalize well to other settings having different characteristics, which is a significant limitation, and more data acquisition can be conducted from households from varying topographical settings.
- 2) This study does not incorporate external factors that might affect the consumption pattern in a household setting. These factors include weather patterns in the geographic location, the economic condition of the residents, or even occupancy patterns. Given the inherent complexity and variability of household energy consumption, the inclusion of these factors external in future research will result in a more robust explainable forecasting workflow.
- 3) XAI frameworks including LIME and SHAP, while effective, do not yield completely transparent interpretable

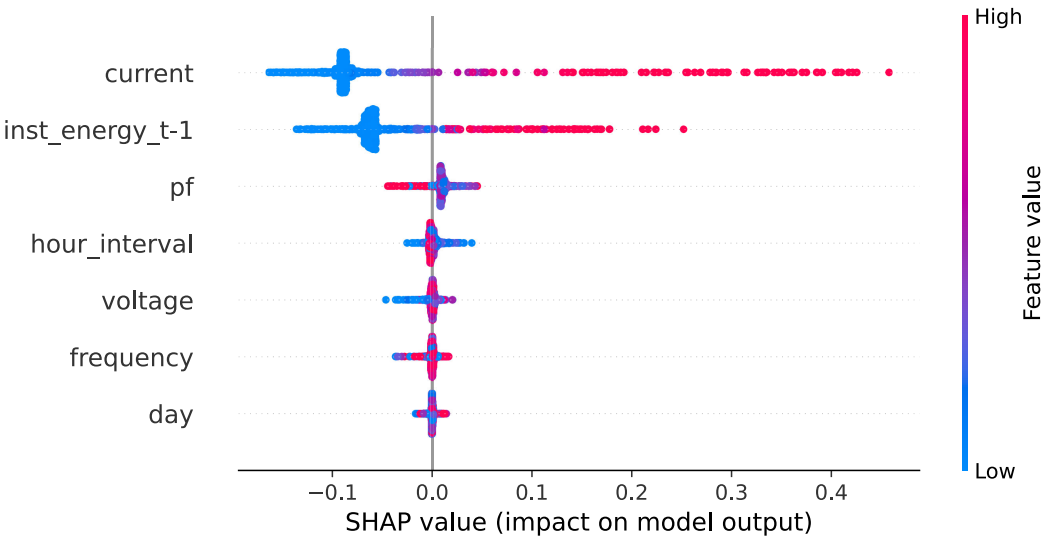
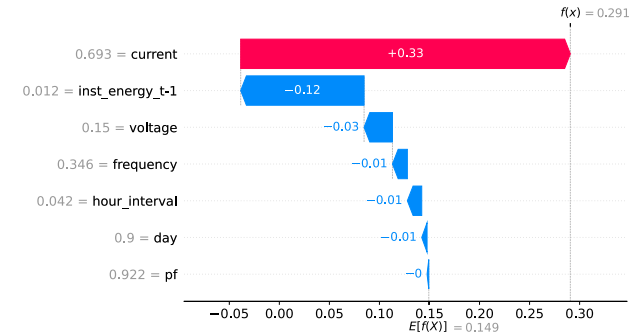
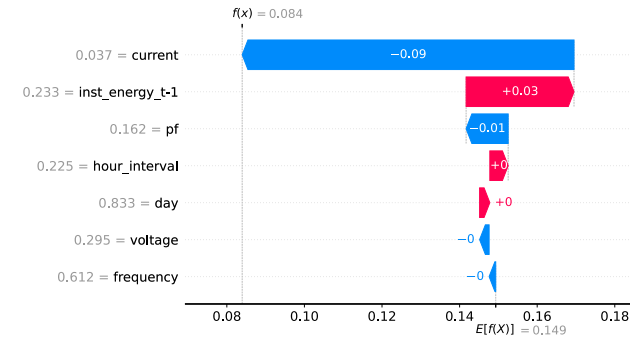


FIGURE 9. SHAP beeswarm plot for interpreting LGBMR results.



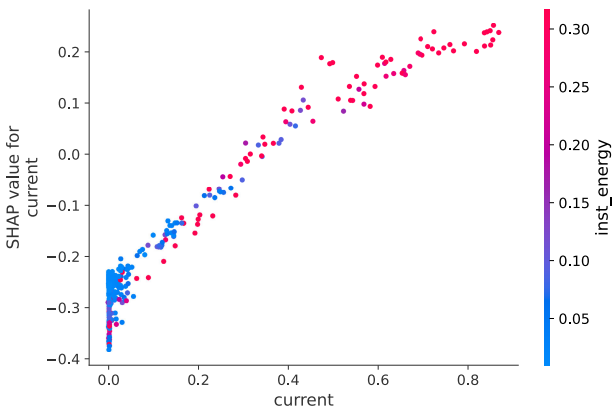
(a) SHAP waterfall plot for an instance where actual value: 0.28315317, predicted value: 0.29074228.



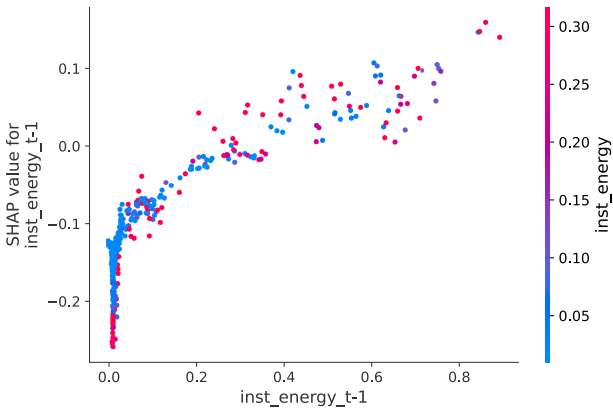
(b) SHAP waterfall plot for an instance where actual value: 0.03100865, predicted value: 0.08395877.

FIGURE 10. SHAP waterfall plots for interpreting individual predictions of the LGBMR model.

models. Instead, they provide slightly gray-box explanations for black-box models. Visualizations such as SHAP waterfall plots still require a baseline understanding of the workings of SHAP, which for a common user might be difficult to grasp.



(a) Dependence plot for current



(b) Dependence plot for inst\_energy\_t-1

FIGURE 11. SHAP dependence plots for two most important features.

VI. CONCLUSION AND FUTURE SCOPE

In this study, we proposed an accurate household electric energy consumption prediction, and robust explanation process by comparing various ML and DL models, and by using

the LIME and SHAP XAI frameworks. Multiple regression models - LGBMR, XGBR, CBR, RFR, LSTM, BiLSTM, and LR were compared using evaluation parameters -  $R^2$ , RMSE, MSE, and MAE. LGBMR produced the most promising results by making the least erroneous predictions on unseen testing data. The analysis of the explanations of the XAI frameworks showed that the *current* and lagged values of energy consumption have the most influence on the model's prediction. The scope of our study lies in its application in households and small buildings, enabling consumers to make informed choices for optimizing energy consumption patterns. Moreover, XAI methods can be seamlessly integrated into existing energy prediction software systems, presenting in-depth information to users in a dashboard format.

While our study provides valuable insights into the interpretability of household energy consumption prediction, several areas for future research and development remain. Firstly, exploring other XAI frameworks beyond LIME and SHAP could offer further insights into the underlying mechanisms of the prediction models. Moreover, investigating the influence of external factors could enhance the accuracy and interpretability of the prediction models. Incorporating these factors into the models and exploring their impact on the prediction would provide a more comprehensive understanding of energy usage patterns.

In conclusion, the application of explainable AI in energy consumption prediction has significant implications for energy management. By improving interpretability and providing transparency, the gap between complex black-box models and human understanding can be bridged.

## ACKNOWLEDGMENT

The authors gratefully acknowledge the support from Pandit Deendayal Energy University (PDEU) to perform this work. The authors would like to express their gratitude to Neel Modi (Department of Information and Communication Technology, School of Technology, PDEU) for his constant support throughout the implementation of the proposed methodology.

## REFERENCES

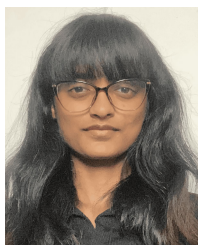
- [1] M. Hind, S. Houde, J. Martino, A. Mojsilovic, D. Piorkowski, J. Richards, and K. R. Varshney, "Experiences with improving the transparency of AI models and services," in *Proc. Extended Abstr. CHI Conf. Human Factors Comput. Syst.*, Apr. 2020, pp. 1–8.
- [2] R. Machlev, L. Heistrene, M. Perl, K. Y. Levy, J. Belikov, S. Mannor, and Y. Levron, "Explainable artificial intelligence (XAI) techniques for energy and power systems: Review, challenges and opportunities," *Energy AI*, vol. 9, Aug. 2022, Art. no. 100169.
- [3] S. Letzgus, P. Wagner, J. Lederer, W. Samek, K.-R. Müller, and G. Montavon, "Toward explainable artificial intelligence for regression models: A methodological perspective," *IEEE Signal Process. Mag.*, vol. 39, no. 4, pp. 40–58, Jul. 2022.
- [4] A. Adadi and M. Berrada, "Peeking inside the black-box: A survey on explainable artificial intelligence (XAI)," *IEEE Access*, vol. 6, pp. 52138–52160, 2018.
- [5] S. M. Lundberg and S.-I. Lee, "A unified approach to interpreting model predictions," in *Proc. Adv. Neural Inf. Process. Syst.*, vol. 30, 2017, pp. 4768–4777.
- [6] M. T. Ribeiro, S. Singh, and C. Guestrin, "Why should I trust you? Explaining the predictions of any classifier," in *Proc. 22nd ACM SIGKDD Int. Conf. Knowl. Discovery Data Mining*, 2016, pp. 1135–1144.
- [7] D. Gunning, M. Stefik, J. Choi, T. Miller, S. Stumpf, and G.-Z. Yang, "XAI—Explainable artificial intelligence," *Sci. Robot.*, vol. 4, no. 37, 2019, Art. no. eaay7120.
- [8] A. B. Arrieta, N. Díaz-Rodríguez, J. Del Ser, A. Bénéttot, S. Tabik, A. Barbado, S. Garcia, S. Gil-Lopez, D. Molina, R. Benjamins, R. Chatila, and F. Herrera, "Explainable artificial intelligence (XAI): Concepts, taxonomies, opportunities and challenges toward responsible AI," *Inf. Fusion*, vol. 58, pp. 82–115, Jun. 2020.
- [9] G. Yenduri and T. R. Gadekallu, "XAI for maintainability prediction of software-defined networks," in *Proc. 24th Int. Conf. Distrib. Comput. Netw.*, Jan. 2023, pp. 402–406.
- [10] X. Wang and M. Yin, "Are explanations helpful? A comparative study of the effects of explanations in AI-assisted decision-making," in *Proc. 26th Int. Conf. Intell. User Interfaces*, Apr. 2021, pp. 318–328.
- [11] T. Sim, S. Choi, Y. Kim, S. H. Youn, D.-J. Jang, S. Lee, and C.-J. Chun, "EXplainable AI (XAI)-based input variable selection methodology for forecasting energy consumption," *Electronics*, vol. 11, no. 18, p. 2947, Sep. 2022.
- [12] Y.-C. Hu, "Electricity consumption prediction using a neural-network-based grey forecasting approach," *J. Oper. Res. Soc.*, vol. 68, no. 10, pp. 1259–1264, Oct. 2017.
- [13] U. Schlegel, H. Arnout, M. El-Assady, D. Oelke, and D. A. Keim, "Towards a rigorous evaluation of XAI methods on time series," in *Proc. IEEE/CVF Int. Conf. Comput. Vis. Workshop (ICCVW)*, Oct. 2019, pp. 4197–4201.
- [14] M. Kuzlu, U. Cali, V. Sharma, and Ö. Güler, "Gaining insight into solar photovoltaic power generation forecasting utilizing explainable artificial intelligence tools," *IEEE Access*, vol. 8, pp. 187814–187823, 2020.
- [15] F. Divina, A. Gilson, F. Gómez-Vela, M. G. Torres, and J. Torres, "Stacking ensemble learning for short-term electricity consumption forecasting," *Energies*, vol. 11, no. 4, p. 949, Apr. 2018.
- [16] J. F. Torres, F. Martínez-Álvarez, and A. Troncoso, "A deep LSTM network for the Spanish electricity consumption forecasting," *Neural Comput. Appl.*, vol. 34, no. 13, pp. 10533–10545, Jul. 2022.
- [17] S. Divya, A. Murthy, S. S. Babu, S. I. Ahmed, and S. R. Dey, "Energy monitoring with trend analysis and power signature interpretation," in *Proc. Emerg. Technol. Data Mining Inf. Secur. (IEMIS)*, vol. 3, Singapore: Springer, 2022, pp. 89–102.
- [18] M. C. Thrun, A. Ultsch, and L. Breuer, "Explainable AI framework for multivariate hydrochemical time series," *Mach. Learn. Knowl. Extraction*, vol. 3, no. 1, pp. 170–204, Feb. 2021.
- [19] H. P. Vinutha, B. Poornima, and B. M. Sagar, "Detection of outliers using interquartile range technique from intrusion dataset," in *Proc. 6th Int. Conf. Inf. Decis. Sci. (FICTA)*, Singapore: Springer, 2018, pp. 511–518.
- [20] M. Ahsan, M. Mahmud, P. Saha, K. Gupta, and Z. Siddique, "Effect of data scaling methods on machine learning algorithms and model performance," *Technologies*, vol. 9, no. 3, p. 52, Jul. 2021.
- [21] A. S. Wilkins, "To lag or not to lag? Re-evaluating the use of lagged dependent variables in regression analysis," *Political Sci. Res. Methods*, vol. 6, no. 2, pp. 393–411, Apr. 2018.
- [22] T. Kubiak and C. Jonas, "Applying circular statistics to the analysis of monitoring data," *Eur. J. Psychol. Assessment*, vol. 23, no. 4, pp. 227–237, Jan. 2007.
- [23] W. McKinney, "Pandas: A foundational Python library for data analysis and statistics," *Python High Perform. Sci. Comput.*, vol. 14, no. 9, pp. 1–9, 2011.
- [24] T. E. Oliphant, *Guide to Numpy*, vol. 1. Austin, TX, USA: Trelgol Publishing, 2006.
- [25] J. Benesty, J. Chen, Y. Huang, and I. Cohen, "Pearson correlation coefficient," in *Noise Reduction in Speech Processing*. Berlin, Germany: Springer, 2009, pp. 1–4.
- [26] A. Liaw and M. Wiener, "Classification and regression by randomForest," *R News*, vol. 2, no. 3, pp. 18–22, 2002.
- [27] S. Siami-Namini, N. Tavakoli, and A. S. Namin, "The performance of LSTM and BiLSTM in forecasting time series," in *Proc. IEEE Int. Conf. Big Data (Big Data)*, Dec. 2019, pp. 3285–3292.
- [28] G. Ke, Q. Meng, T. Finley, T. Wang, W. Chen, W. Ma, Q. Ye, and T.-Y. Liu, "LightGBM: A highly efficient gradient boosting decision tree," in *Proc. Adv. Neural Inf. Process. Syst.*, vol. 30, 2017, pp. 3149–3157.



- [29] L. Prokhorenkova, G. Gusev, A. Vorobev, A. V. Dorogush, and A. Gulin, "CatBoost: Unbiased boosting with categorical features," in *Proc. Adv. Neural Inf. Process. Syst.*, vol. 31, 2018, pp. 6639–6649.
- [30] T. Chen and C. Guestrin, "XGBoost: A scalable tree boosting system," in *Proc. 22nd ACM SIGKDD Int. Conf. Knowl. Discovery Data Mining*, Aug. 2016, pp. 785–794.
- [31] C. Ding, X. Cao, and P. Naess, "Applying gradient boosting decision trees to examine non-linear effects of the built environment on driving distance in Oslo," *Transp. Res. A, Policy Pract.*, vol. 110, pp. 107–117, Apr. 2018.
- [32] G. Yenduri and T. R. Gadekallu, "A multiple criteria decision analysis based approach to remove uncertainty in SMP models," *Sci. Rep.*, vol. 12, no. 1, p. 22386, Dec. 2022.
- [33] L. E. Melkumova and S. Y. Shatskikh, "Comparing ridge and LASSO estimators for data analysis," *Proc. Eng.*, vol. 201, pp. 746–755, Jan. 2017.
- [34] D. P. Kingma and J. Ba, "Adam: A method for stochastic optimization," 2014, *arXiv:1412.6980*.
- [35] G. Yenduri and V. Naralasetti, "A nonlinear weight-optimized maintainability index of software metrics by grey wolf optimization," *Int. J. Swarm Intell. Res.*, vol. 12, no. 2, pp. 1–21, Apr. 2021.
- [36] D. Chicco, M. J. Warrens, and G. Jurman, "The coefficient of determination R-squared is more informative than SMAPE, MAE, MAPE, MSE and RMSE in regression analysis evaluation," *PeerJ Comput. Sci.*, vol. 7, p. e623, Jul. 2021.
- [37] E. Winter, "The Shapley value," in *Handbook of Game Theory With Economic Applications*, vol. 3. Amsterdam, The Netherlands: North-Holland, 2002, pp. 2025–2054.



**AAKASH BHANDARY** (Student Member, IEEE) is currently pursuing the B.Tech. degree in computer engineering with Pandit Deendayal Energy University, Gandhinagar, India. He was an Intern with Aeon Software Pvt., Ltd., India. His research interests include applied machine learning, deep learning, explainable AI, and large language models.



**VRUTI DOBARIYA** is currently pursuing the B.Tech. degree in computer engineering with Pandit Deendayal Energy University, Gandhinagar, India. She was an Intern with DhiWise, India. Her research interests include generative AI, machine learning, deep learning, natural language processing, and large language models.



**GOKUL YENDURI** received the M.Tech. degree in IT from Vellore Institute of Technology, in 2013, where he recently submitted his Ph.D. degree. He is an Assistant Professor with VIT-AP University. He is a Senior Research Fellow with DIVERSASIA Project, co-funded by the Erasmus+ Program of the European Union in the past. He has attended several national and international conferences, workshops, and guest lectures. He has published articles in peer-reviewed international journals. His research interests include machine learning and predictive analysis, software engineering, assistive technologies, and metaverse. He is acting as a reviewer of many prestigious peer-reviewed international journals.



**RUTVIJ H. JHAVERI** (Senior Member, IEEE) received the Ph.D. degree in computer engineering, in 2016. He is currently an experienced Educator and a Researcher with the Department of Computer Science and Engineering, Pandit Deendayal Energy University, Gandhinagar, India. He conducted his Postdoctoral Research with the Delta-NTU Corporate Laboratory for Cyber-Physical Systems, Nanyang Technological University, Singapore. He has authored more than 150 articles, including IEEE/ACM TRANSACTIONS and flagship IEEE/ACM conferences. Moreover, he has several national and international patents and copyrights to his name. He is also co-investigating a funded project from GUJCOST. His research interests include cyber security, the IoT systems, SDN, and smart healthcare. He is an Editorial Board Member in various journals of repute, including IEEE TRANSACTIONS ON INDUSTRIAL INFORMATICS and *Scientific Reports*. He serves as a reviewer for several international journals and also as an advisory/TPC member in renowned international conferences. He also possesses memberships of various technical bodies, such as ACM, CSI, and ISTE. He is the Coordinator of Smart Cities Air Quality Network (SCAN). Moreover, he has been a member of the Advisory Board in Symbiosis Institute of Digital and Telecom Management and other reputed universities, since 2022. He is an editorial board member in several Springer and Hindawi journals. He served as a Committee Member for "Smart Village Project"-Government of Gujarat, at the district level, in 2017. In 2017, he was awarded with Prestigious Pedagogical Innovation Award by Gujarat Technological University. He was ranked among top 2% scientists around the world in 2021 and 2022. He has more than 3200 Google Scholar citations with H-index of 31.



**SAIKAT GOCHHAIT** (Senior Member, IEEE) teaches at the Symbiosis Institute of Digital and Telecom Management, Symbiosis International Deemed University, Pune, India, and Neurosciences Research Institute-Samara State Medical University, Russia. He is a Ph.D and Post-Doctoral Fellow from the UEx, Spain, and National Dong Hwa University, Taiwan. He was Awarded DITA and MOFA Fellowship in 2017 and 2018. His research publication with foreign authors is indexed in Scopus, ABDC, and Web of Science.



**FRANCESCO BENEDETTO** (Senior Member, IEEE) has been the Chair of the IEEE 1900.1 Standard "Definitions and Concepts for Dynamic Spectrum Access: Terminology Relating to Emerging Wireless Networks, System Functionality, and Spectrum Management," since 2016. He has been the Leader of the WP 3.5 on "Development of Advanced GPR Data Processing Technique" of the European COST Action TU1208—Civil Engineering Applications of Ground Penetrating Radar. He is the General Co-Chair of the IEEE 43rd International Conference on Telecommunications and Signal Processing (TSP 2020) and the General Chair of the Series of International Workshops on Signal Processing for Secure Communications (SP4SC 2014, 2015, and 2016). He is an Associate Editor of IEEE Access, an Editor of the IEEE SDN Newsletter, an Associate Editor of the *AEU-International Journal of Electronics and Communications* (Elsevier), the Editor-in-Chief of the International Journal *Recent Advances in Computer Science and Communications* (Bentham), and the Lead Guest Editor of the Special Issue on "Advanced Ground Penetrating Radar Signal Processing Techniques" for the *Signal Processing* (Elsevier). He also served as a reviewer for several IEEE TRANSACTIONS, IET proceedings, EURASIP, and Elsevier journals, and a TPC Member for several IEEE international conferences and symposia in the same fields.

...